Mainlobe Interference Suppression Based on Compressive Sensing and Covariance Matrix Reconstruction

Xinpeng ZHAO, Aifeng REN

Shool of Electronic Engineering, Xidian University, Xi'an 710071, China

xinpengzhao@stu.xidian.edu.cn, afren@mail.xidian.edu.cn

Abstract. *When mainlobe interference exists in space, the traditional anti-interference methods have problems such as peak offset and the performance of sidelobe interference suppression reduction. To solve the above problems, this paper proposes a mainlobe interference suppression method based on compressive sensing and covariance matrix reconstruction. Firstly, an improved compressive sensing algorithm is proposed to accurately estimate the Direction Of Arrival of sources, and then the signal steering vectors and signal subspaces can be established. The mainlobe interference can be suppressed by establishing an oblique projection operator through signal subspaces. Meanwhile, the sidelobe-interference-noise covariance matrix can be reconstructed by the steering vectors, and then the adaptive weight vector is obtained. Simulation results show that the proposed method can form a more robust beam pattern and has better output performance. The proposed method is still effective when the desired signal exists in the received signal.*

Keywords

Mainlobe interference suppression, compressive sensing, covariance matrix reconstruction, Direction Of Arrival (DOA)

1. Introduction

With the rapid development of jamming technology, the electromagnetic environment faced by the radar in the field of electronic countermeasures (ECM) is increasingly complex [1], [2]. Typical adaptive beamforming (ADBF) methods such as adaptive sidelobe cancellation (ASLC) can effectively suppress sidelobe interference. But if the interference falls into the mainlobe range, the conventional adaptive beamforming methods will form a zero notch in the mainlobe of the array pattern, resulting in the deviation and deformation of the main beam, and will raise the sidelobe level of the beam. In addition, the suppression of mainlobe interference by conventional methods will also affect the subsequent signal processing processes, such as increasing false alarm probability and decreasing angle measurement accuracy in radar detection [3].

How to effectively suppress the mainlobe interference has become a research hotspot in radar countermeasures. In [4], [5], the polarization-sensitive array is used to effectively improve the anti-mainlobe interference ability of the radar, but the methods require radar to have the capability of measuring polarization information. In [6], [7], blind source separation (BSS) is adopted to separate the target signal and filter out the mainlobe interference, but the accurate directions of signals could not be obtained, so the methods have a certain amount of errors. The method based on eigen-projection preprocessing (EMP) [8] can obtain a distortion-free directional pattern, but there is still the problem of peak offset. Based on the EMP method, the eigen-projection and covariance matrix reconstruction (EMP-CMR) method is proposed in [9], which can eliminate the influence of mainlobe interference on the adaptive weight vector by reconstructing the covariance matrix and effectively reduce the peak offset. Reference [10] is also based on the EMP method, eigen-projection algorithm and similarity constraints are used to successfully suppress the multi-mainlobe interferences. However, the methods proposed in [8–10] all suppose that there is no desired signal in the received training data, and only exist interferences, which have limitations in practical engineering applications.

In order to reconstruct the interference-noise covariance matrix (INCM) when there exists the desired signal in the received training data, some robust adaptive beamforming methods [11], [12] are proposed. Reference [13], [14] suppress the mainlobe interference by eigen-oblique projection, and achieve outstanding output performance. But the methods of reference [13], [14] assumes that the direction of the desired signal is known, and this information cannot be obtained in advance. Reference [15] distributed received signals into different angular sectors, by using the Capon power spectrum to make integration operation in the corresponding sector, the sidelobe-interference-noise covariance matrix (SINCM) can be reconstructed finally. In [16], the DOAs of signals are obtained by the IAA spectrum estimation method, and then the SINCM is obtained by the combination and accumulation of interference power and interference steering

vectors (SV). However, the integration operation requires a significant amount of computational complexity, and the spectrum estimation method suffers from energy leakage. In [17], [18], SINCM is reconstructed by compressive sensing, which takes advantage of the sparse characteristics of spatial signals, effectively reducing the computational complexity compared with the integration operation. However, the DOA estimation methods in [17] and [18] are the Capon space spectrum and MUSIC algorithm respectively. When the power of mainlobe interference is much larger than the power of the desired signal and the number of snapshots is not large enough, the direction of the desired signal is difficult to be obtained from the power spectrum, which will affect subsequent operations.

In recent years, the compressive sensing theory has been increasingly applied in signal processing [19], [20]. Numerous researchers have incorporated the concept of sparsity into the DOA estimation of signals [21], [22], which has shown superior performance than conventional methods. This paper proposes an anti-mainlobe interference method based on compressive sensing and covariance matrix reconstruction. The purpose is to effectively suppress the interferences when the mainlobe interference and the desired signal both exist in the training data. By the compressive sensing algorithm, the DOAs of signals can be accurately estimated, and the SINCM can be further reconstructed. Finally, the oblique projection operator and the adaptive weight vector are used to suppress the mainlobe interference and sidelobe interference respectively. Theoretical analysis and simulation results verify the effectiveness of the proposed method.

The rest of this paper is structured as follows: In Sec. 2 the adaptive array signal model is introduced. In Sec. 3, an improved algorithm based on the orthogonal matching pursuit algorithm is proposed, and the processions of calculating the oblique projection operator and reconstructing the covariance matrix are introduced. Some simulation results are provided in Sec. 4 and conclusions are given in Sec. 5.

2. Signal Model

Consider a uniform linear array (ULA) consisting of M omnidirectional antenna elements which receive $p + 1$ uncorrelated far-field narrowband signals in the space, including one expected signal and p interference signals, where $p + 1 < M$. The received signal by the array antenna at the k-th snapshot can be expressed as:

$$\mathbf{x}(k) = \mathbf{x}_s(k) + \mathbf{x}_i(k) + \mathbf{n}(k) = \sum_{i=0}^{p} \mathbf{a}(\theta_i) s_i(k) + \mathbf{n}(k) \quad (1)$$

where $\mathbf{x}_s(k)$ and $\mathbf{x}_i(k)$ are independent components of the desired signal and interferences, respectively. $\mathbf{n}(k)$ is the $M \times 1$ dimension Gaussian white noise vector with zero means. $\theta_i, i = 0, 1, \ldots, p$ stands for the DOA of the i-th signal, in which θ_0 and θ_1 denote the directions of the desired signal

and mainlobe interference, respectively. $\mathbf{a}(\theta_i)$ and $s_i(k)$ denote the steering vector and the complex envelope of the i-th signal, respectively. The theoretical covariance matrix of the received signal is expressed as:

$$\mathbf{R} = \mathrm{E}\{\mathbf{X}\mathbf{X}^H\} = \mathbf{A}\mathbf{R}_s\mathbf{A}^H + \sigma_n^2\mathbf{I} \quad (2)$$

where $\mathbf{X}$ is the sample matrix of the received signal, $\mathrm{E}\{\cdot\}$ denotes the statistical expectation and $(\cdot)^H$ denotes the Hermitian transpose. $\mathbf{A} = [\mathbf{a}(\theta_0), \mathbf{a}(\theta_1), \ldots, \mathbf{a}(\theta_p)] \in C^{M \times (p+1)}$ is the array manifold matrix, $\mathbf{R}_s$ denotes the covariance matrix of the desired signal and interferences. σ_n^2 is the noise power. The output of array at the k-th snapshot can be calculated as:

$$y(k) = \omega^H \mathbf{x}(k). \quad (3)$$

Here, $\omega = [\omega_1, \ldots, \omega_M]^T$ is the adaptive beamformer weight vector, $(\cdot)^T$ denote the transpose. The optimal weight vector is the solution of the minimum variance distortion-less response (MVDR) beamformer problem, which is given by:

$$\omega_{\mathrm{opt}} = \frac{\mathbf{R}_{i+n}^{-1}\mathbf{a}(\theta_0)}{\mathbf{a}(\theta_0)^H\mathbf{R}_{i+n}^{-1}\mathbf{a}(\theta_0)} \quad (4)$$

where $\mathbf{R}_{i+n} = \mathrm{E}\{(\mathbf{x}_i(k) + \mathbf{n}(k))(\mathbf{x}_i(k) + \mathbf{n}(k))^H\} \in C^{M \times M}$ is the INCM of the received signal. Since $\mathbf{R}_{i+n}$ is unavailable in general, it's usually replaced by the sample covariance matrix $\hat{\mathbf{R}} = 1/K \sum_{k=1}^{K} \mathbf{x}(k)\mathbf{x}^H(k)$ with K training snapshots, $\hat{\mathbf{R}}$ is also the estimate of $\mathbf{R}$. $\hat{\mathbf{R}}$ can be eigen-decomposed as:

$$\hat{\mathbf{R}} = \sum_{i=1}^{M} \lambda_i \mathbf{u}_i \mathbf{u}_i^H \quad (5)$$

where $\lambda_1 \geq \cdots \geq \lambda_{p+1} \geq \cdots \geq \lambda_M$ are the eigenvalues of $\hat{\mathbf{R}}$ in the descending order, and $\mathbf{u}_i$ is the corresponding eigenvector. Since the signal power is obviously greater than the noise power, and there are $p + 1$ sources in the space, hence there are $p + 1$ large eigenvalues among the M eigenvalues. $\mathbf{u}_1, \mathbf{u}_2, \ldots, \mathbf{u}_{p+1}$ form the joint subspace of desired signal and interferences, which is the same as that formed by $\mathbf{a}(\theta_0), \mathbf{a}(\theta_1), \ldots, \mathbf{a}(\theta_p)$, and $\mathbf{u}_{p+2}, \mathbf{u}_{p+3}, \ldots, \mathbf{u}_M$ form the noise subspace. The obtained adaptive beamformer $\omega_{\mathrm{SMI}} = \hat{\mathbf{R}}^{-1}\mathbf{a}(\theta_0)/\mathbf{a}(\theta_0)^H\hat{\mathbf{R}}^{-1}\mathbf{a}(\theta_0)$ is called the sample matrix inversion (SMI) adaptive beamformer.

The corresponding Capon spatial spectrum distribution can be calculated as:

$$\hat{P}_{\mathrm{Capon}}(\theta) = \frac{1}{\mathbf{d}^H(\theta)\hat{\mathbf{R}}^{-1}\mathbf{d}(\theta)} \quad (6)$$

where $\mathbf{d}(\theta)$ is the steering vector associated with the array structure and the direction is θ. However, when the training data contains the desired signal, the SMI beamformer is actually the minimum power distortionless response (MPDR) beamformer instead of the MVDR beamformer. MPDR beamformer is more sensitive to the error of the steering

vector than MVDR beamformer and will affect the performance of beamforming. Additionally, when there is a mainlobe interference in training data, nulls will be formed in the direction of mainlobe interference, which leads to the reduction of the desired signal power and more degradation of the performance of beamforming.

3. Proposed Method

3.1 Compressive Sensing

Suppose that there exists a complex signal $\mathbf{x} = [x_1, \ldots, x_n]^T$ that can be represented by a linear combination of a sparse basis matrix $\mathbf{\Psi} \in C^{n \times n}$, that is $\mathbf{x} = \mathbf{\Psi s}$, where $\mathbf{s}$ is an n-dimensional signal with k-sparse($k \ll n$). At this point, $\mathbf{x}$ is measured by a matrix $\mathbf{\Phi} \in C^{m \times n} (m \ll n)$ that is uncorrelated with $\mathbf{\Psi}$, as shown in Fig. 1. The linear projection measurement of the signal $\mathbf{x}$ under $\mathbf{\Phi}$ can be obtained as:

$$\mathbf{y} = \mathbf{\Phi x} = \mathbf{\Phi \Psi s} = \mathbf{\Theta s} \tag{7}$$

where $\mathbf{\Phi}$ is the measurement matrix, $\mathbf{\Theta} = \mathbf{\Phi \Psi}$ is the $m \times n$ dimension matrix, which represents the generalized measurement matrix and is called the perception matrix. Therefore, $\mathbf{y}$ can be regarded as the linear measurement of sparse signal $\mathbf{s}$ under the perception matrix $\mathbf{\Theta}$. If the perception matrix $\mathbf{\Theta}$ meets the sparse reconstruction conditions such as RIP [23], then the sparse signal $\mathbf{s}$ can be reconstructed with a very high probability by solving the following 0-norm problem:

$$\begin{cases} \hat{\mathbf{s}} = \arg \min \|\mathbf{s}\|_0, \\ \text{s.t. } \mathbf{\Theta s} = \mathbf{y}. \end{cases} \tag{8}$$

The initial signal $\mathbf{x}$ can be recovered by inverse sparse basis matrix transformation.

In the array model, the space from $-90°$ to $90°$ is uniformly divided into N angles $\{\theta_1, \theta_2, \ldots, \theta_N\}$, and assuming that each element has a potential signal source, then the spatial source signal vector can be represented as $\mathbf{S} = [s_1, s_2, \ldots, s_N]^T$, and the angle grid $\Delta = 180°/(N-1)$. In fact, there are only P ($P \ll N$) signal sources in N directions, so only P signals corresponding to directions in $\mathbf{S}$ have non-zero elements and there are all zero in other $N-P$ positions. That is, $\mathbf{S}$ is P-sparse. The array DOA estimation model represented by the sparse signal is:

$$\mathbf{Y} = \tilde{\mathbf{A}} \mathbf{S} + \mathbf{n} \tag{9}$$

where $\mathbf{Y} = [Y_1, Y_2, \ldots, Y_N]^T$ indicates the received signal at a certain time. $\tilde{\mathbf{A}}$ is the extended array manifold matrix, which can be expressed as $\tilde{\mathbf{A}} = [\mathbf{a}_1, \mathbf{a}_2, \ldots, \mathbf{a}_N] \in C^{M \times N}$, where $\mathbf{a}_i (i = 1, 2, \ldots, N)$ is the steering vector of signal with the direction θ_i. Since $\mathbf{S}$ is a sparse signal, thus $\tilde{\mathbf{A}}$ is both a measurement matrix and a perception matrix. In the sparse reconstruction model, $\tilde{\mathbf{A}}$ is also called the overcomplete dictionary, $\mathbf{a}_i$ is called the atom of $\tilde{\mathbf{A}}$. $\mathbf{n}$ is the noise of the array.
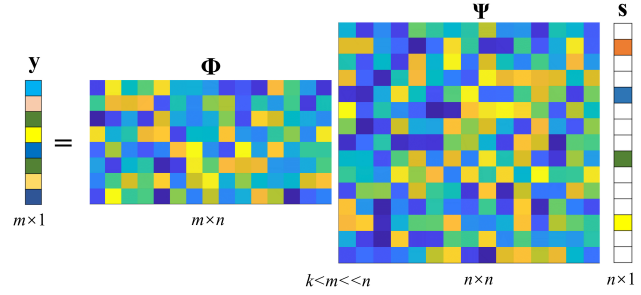
Fig. 1. The compressed sampling process of sparse signal.

The DOA estimation in the compressive sensing framework is to reconstruct the signal vector $\mathbf{S}$ under the condition of considering noise by the known array received signal $\mathbf{Y}$ and measurement matrix $\tilde{\mathbf{A}}$, then the DOA of the signal can be determined according to the correspondence between the N units divided in space and the nonzero position of the sparse signal $\mathbf{S}$. Greedy algorithms have low computational complexity and fast running speed, so they are widely used in the field of compressive sensing, one of the most representative is the Orthogonal Matching Pursuit (OMP) algorithm [24]. Other classical greedy algorithms have improvement on the method of atomic selection, such as ROMP, CoSaMP and SP. But there exists some correlation between the columns of $\tilde{\mathbf{A}}$, which lead to other algorithms are not as steady as OMP in the domain of DOA estimation [25]. The steps of OMP Algorithm are shown in Algorithm 1.

Algorithm 1 OMP Algorithm.

Input: measurement matrix $\tilde{\mathbf{A}}$, data vector $\mathbf{Y}$, sparsity P
Output: P-sparse signal $\hat{\mathbf{S}}$
1: Initialize the residual $\mathbf{r}_0 = \mathbf{Y}$, index set $\mathbf{\Lambda}_0 = \varnothing$, atoms set $\mathbf{A}_0 = \varnothing$, iteration counter $t = 1$
2: $\lambda_t = \arg \max_{i=1,\ldots,N} |\langle \mathbf{r}_{t-1}, \mathbf{a}(\theta_i) \rangle|$, $\mathbf{a}_{\lambda_t}$ is the λ_t-th atom of $\tilde{\mathbf{A}}$
3: $\mathbf{\Lambda}_t = \mathbf{\Lambda}_{t-1} \bigcup \{\lambda_t\}$, $\mathbf{A}_t = \mathbf{A}_{t-1} \bigcup \{\mathbf{a}_{\lambda_t}\}$
4: Find the least squares solution of $\mathbf{Y} = \mathbf{A}_t \cdot \mathbf{S}$, obtain $\mathbf{S}_t = (\mathbf{A}_t^T \mathbf{A}_t)^{-1} \mathbf{A}_t^T \mathbf{Y}$
5: Update residual $\mathbf{r}_t = \mathbf{Y} - \mathbf{A}_t \cdot \mathbf{S}_t$, $t = t + 1$
6: If $t \leq P$, return to Step 2.
7: $\hat{\mathbf{S}}$ has nonzero indices at the components listed in $\mathbf{\Lambda}_P$, the t-th nonzero value of $\hat{\mathbf{S}}$ is the t-th component of $\mathbf{S}_P$

Here the sparsity P is the number of sources, which can be obtained from the number of large eigenvalues of the sampling covariance matrix $\hat{\mathbf{R}}$. The linear combination of the P-dimensional vector $\mathbf{S}_P$ and atoms set $\mathbf{A}_P$ can approximate $\mathbf{Y}$ in consideration of noise, where $\mathbf{A}_P = [\mathbf{a}_{\lambda_1}, \mathbf{a}_{\lambda_2}, \ldots, \mathbf{a}_{\lambda_P}]$ and $\mathbf{S}_P = [s_{\lambda_1}, s_{\lambda_2}, \ldots, s_{\lambda_P}]^T$. Then we have:

$$\mathbf{Y} \approx \mathbf{A}_P \mathbf{S}_P = s_{\lambda_1} \mathbf{a}_{\lambda_1} + s_{\lambda_2} \mathbf{a}_{\lambda_2} + \cdots + s_{\lambda_P} \mathbf{a}_{\lambda_P}. \tag{10}$$

If the reconstruction is successful, that is, the correct atoms are selected during each iteration. Due to the noise power is far less than the signal power, the power of the final residual $\|\mathbf{r}_P\|_2 = \|\mathbf{Y} - \mathbf{A}_P \mathbf{S}_P\|_2$ should be a small value, where $\| \cdot \|_2$ refers to the Euclidean norm of a vector. If the wrong atom $\mathbf{a}_{\lambda_i}$ is chosen at the i-th iteration, which will make the recovered sparse signal far from the original signal, leading to the failure of reconstruction. In this case, $\mathbf{Y}$ cannot

be approximated by the wrong $\mathbf{A}_P$ and $\mathbf{S}_P$, so the residual energy $||r_P||_2$ will be a relatively large value. When there are two or more signals in the training data with close direction, such as mainlobe interference and the desired signal, the correlation between their corresponding steering vectors is strong, and the OMP algorithm may select the wrong atoms in the iteration process, resulting in reconstruction failure.

Suppose that the serial number chosen in the i-th iteration is λ_i, and the corresponding atoms and signal components are $\mathbf{a}_{\lambda_i}$ and s_{λ_i}, respectively. And the real serial numbers, atoms and signal components are $\tilde{\lambda}_i$, $\mathbf{a}_{\tilde{\lambda}_i}$ and $s_{\tilde{\lambda}_i}$, respectively. Consider the deviation caused by the current component:

$$\left\|\mathbf{r}_{\lambda_i}\right\|_2 = \left\|s_{\tilde{\lambda}_i}\mathbf{a}_{\tilde{\lambda}_i} - s_{\lambda_i}\mathbf{a}_{\lambda_i}\right\|_2. \tag{11}$$

Search around λ_i, and assume that the calculated signal component is s_i when $\tilde{\lambda}_i$ is searched. In general, $s_i \approx s_{\tilde{\lambda}_i}$, so the deviation $\left\|\mathbf{r}_{\lambda_i}\right\|_2 = (s_{\tilde{\lambda}_i} - s_i)\left\|\mathbf{a}_{\tilde{\lambda}_i}\right\|_2 \approx 0$. Thus, the selected atoms can be modified by minimizing the final residual, so that the correct atoms can be searched, and the probability of DOA success estimation can be significantly improved.

Given this, we propose an improved Orthogonal Matching Pursuit algorithm based on Testing Residuals (TROMP), which checks the element (atomic serial-number) of $\mathbf{\Lambda}_P$, the selected atomic serial numbers which satisfy the conditions are replaced with the atomic serial number near to them respectively that can minimize the residual, the replacements are executed one by one according to the order of atom selection. The main steps of the TROMP algorithm have been summarized in Algorithm 2 and Fig. 2 shows the modified process of serial numbers.

In the TROMP algorithm, the threshold factor m is a small constant (for example, $m = 3$ will be used in our simulations), which is related to the discriminant condition

---

Algorithm 2 TROMP Algorithm.

Input: measurement matrix $\tilde{\mathbf{A}}$, data vector $\mathbf{Y}$, sparsity P, threshold factor m

Output: P-sparse signal $\hat{\mathbf{S}}$

1: Initialize the residual $\mathbf{r}_0 = \mathbf{Y}$, index set $\mathbf{\Lambda}_0 = \varnothing$, atoms set $\mathbf{A}_0 = \varnothing$, iteration counter $t = 1$, interval factor $c = 1/\Delta$
2: Use OMP catch $\mathbf{\Lambda}_P$ and $\mathbf{r}_P$
3: Check the element of $\mathbf{\Lambda}_P$. Suppose that for λ_i, there exists $\lambda_g \in \mathbf{\Lambda}_P (g > i)$ which satisfies $|\lambda_g - \lambda_i| \leq 2m \cdot c$, then enter Step 4.
4: Take out $2m$ serial numbers near λ_i by interval $\pm k \cdot c$ $(k = 1, 2, \ldots, m)$, mark them as $\delta_j (j = 1, 2, \ldots, 2m)$, initialize $j = 1$
5: Replace λ_i with δ_j, $\mathbf{\Lambda} = \{\lambda_1, \lambda_2, \ldots, \lambda_{i-1}, \delta_j, \ldots, \lambda_P\}$, $\mathbf{A}_i = \{\mathbf{a}_{\mathbf{\Lambda}}\}$, $\mathbf{S}_i = (\mathbf{A}_i^{\mathrm{T}}\mathbf{A}_i)^{-1}\mathbf{A}_i^{\mathrm{T}}\mathbf{Y}$, residual $\mathbf{R}_i = \mathbf{Y} - \mathbf{A}_i \cdot \mathbf{S}_i$, update $\mathbf{r}_P$ to $\mathbf{R}_i$ and record δ_j if $||\mathbf{R}_i||_2 < ||\mathbf{r}_P||_2$. $j = j + 1$, repeat Step 5 if $j \leq 2m$
6: if δ_j is recorded, replace $\lambda_i \in \mathbf{\Lambda}$ with δ_j. $i = i + 1$, return step 4 if $i \leq P$
7: Obtain the modified index set $\mathbf{\Lambda}$, atoms set $\mathbf{A}_P = \{\mathbf{a}_{\mathbf{\Lambda}}\}$, $\mathbf{S} = (\mathbf{A}_P{}^{\mathrm{T}}\mathbf{A}_P)^{-1}\mathbf{A}_P{}^{\mathrm{T}}\mathbf{Y}$
8: $\hat{\mathbf{S}}$ has nonzero indices at the components listed in $\mathbf{\Lambda}$, the t-th nonzero value of $\hat{\mathbf{S}}$ is the t-th component of $\mathbf{S}$
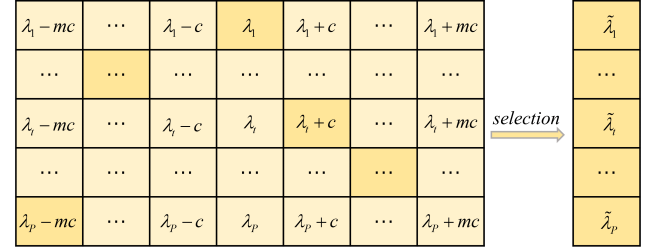
Fig. 2. The modified process of serial numbers.

of the signals with close direction and the correction range of the atomic serial number. The idea of testing residuals does not take the DOA estimated by the OMP algorithm as the final results, but in the near range of each DOA estimation to search for the optimal value, so the DOA estimation is more likely to be correct.

The desired signal is assumed to be located in the known angular sector where is no interference, the DOA of the desired signal can be determined by looking for the peak of the spatial spectrum corresponding to $\hat{\mathbf{S}}$ in the angular sector. The interference whose direction is close to the desired signal is the mainlobe interference, and the rest is the sidelobe interference.

3.2 SINCM Reconstruction

The DOA of each signal has been estimated by TROMP, then the array manifold matrix can be expressed as $\hat{\mathbf{A}} = [\mathbf{a}(\hat{\theta}_0), \mathbf{a}(\hat{\theta}_1), \ldots, \mathbf{a}(\hat{\theta}_p)]$, where $\mathbf{a}(\hat{\theta}_0)$ and $\mathbf{a}(\hat{\theta}_1)$ denote the steering vectors of the desired signal and mainlobe interference respectively. Convert (2) into:

$$\hat{\mathbf{R}} = \hat{\mathbf{A}}\mathbf{R}_s\hat{\mathbf{A}}^{\mathrm{H}} + \hat{\sigma}_n^2\mathbf{I} \tag{12}$$

where $\hat{\sigma}_n^2$ is the estimated noise power, which can be obtained by averaging the $M - p - 1$ small eigenvalues of $\hat{\mathbf{R}}$:

$$\hat{\sigma}_n^2 = \frac{\lambda_{p+2} + \cdots + \lambda_M}{M - p - 1}. \tag{13}$$

When the signals are uncorrelated, $\mathbf{R}_s$ is a diagonal matrix whose elements on the main diagonal represent the power of each signal, respectively. The least squares solution of $\mathbf{R}_s$ is:

$$\mathbf{R}_s = \hat{\mathbf{A}}^+ (\hat{\mathbf{R}} - \hat{\sigma}_n^2\mathbf{I})(\hat{\mathbf{A}}^{\mathrm{H}})^+ \tag{14}$$

where the pseudo-inverse of $\hat{\mathbf{A}}$ is defined as $\hat{\mathbf{A}}^+ = (\hat{\mathbf{A}}^{\mathrm{H}}\hat{\mathbf{A}})^{-1}\hat{\mathbf{A}}^{\mathrm{H}}$. When the number of snapshots is small, there may be redundant correlation between the signals, which makes $\mathbf{R}_s$ have nonzero values in positions other than the main diagonal and leads to reduction of the anti-interference performance. Therefore, the elements outside the main diagonal of $\mathbf{R}_s$ should be discarded, and the power of each signal can be obtained from the main diagonal of $\mathbf{R}_s$ according to the construction order of $\hat{\mathbf{A}}$. The power set can be expressed as $\hat{\sigma}_0^2, \hat{\sigma}_1^2, \ldots, \hat{\sigma}_p^2$, where $\hat{\sigma}_0^2$ and $\hat{\sigma}_1^2$ denote the powers of the
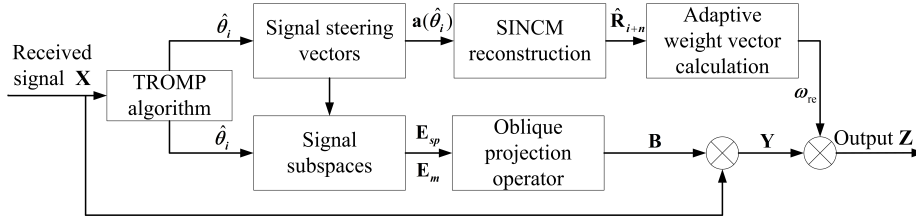
Fig. 3. The processing block diagram of the proposed method.

desired signal and mainlobe interference respectively. Then the SINCM can be reconstructed as:

$$\hat{\mathbf{R}}_{i+n} = \sum_{i=2}^{p} \hat{\sigma}_i^2 \mathbf{a}(\hat{\theta}_i) \mathbf{a}(\hat{\theta}_i)^{\mathrm{H}} + \hat{\sigma}_n^2 \mathbf{I}. \tag{15}$$

There are no mainlobe interference and desired signal components in $\hat{\mathbf{R}}_{i+n}$, so by using $\hat{\mathbf{R}}_{i+n}$ to calculate the adaptive weight vector, the sidelobe interference can be effectively suppressed.

3.3 Oblique Projection Filtering

The oblique projection filter is used to suppress the mainlobe interference. Considering two full-column-rank matrices $\mathbf{S} \in C^{a \times b}$ and $\mathbf{H} \in C^{a \times c}$, if $b + c < a$ and the column vectors of $\mathbf{S}$ and $\mathbf{H}$ are linearly independent, the subspaces $\langle \mathbf{S} \rangle$ and $\langle \mathbf{H} \rangle$ formed by $\mathbf{S}$ and $\mathbf{H}$ have no intersection. Then the oblique projection operator $\mathbf{B_{SH}}$ to the subspace $\langle \mathbf{S} \rangle$ along the direction parallel to the subspace $\langle \mathbf{H} \rangle$ is defined as:

$$\begin{aligned}\mathbf{B_{SH}} &= \begin{bmatrix} \mathbf{S} & \mathbf{H} \end{bmatrix} \begin{bmatrix} \mathbf{S}^{\mathrm{H}}\mathbf{S} & \mathbf{S}^{\mathrm{H}}\mathbf{H} \\ \mathbf{H}^{\mathrm{H}}\mathbf{S} & \mathbf{H}^{\mathrm{H}}\mathbf{H} \end{bmatrix}^{\dagger} \begin{bmatrix} \mathbf{S}^{\mathrm{H}} \\ \mathbf{H}^{\mathrm{H}} \end{bmatrix} \\ &= \mathbf{S}(\mathbf{S}^{\mathrm{H}}\mathbf{P}_{\mathbf{H}}^{\perp}\mathbf{S})^{-1}\mathbf{S}^{\mathrm{H}}\mathbf{P}_{\mathbf{H}}^{\perp}\end{aligned} \tag{16}$$

where $[\cdot]^{\dagger}$ means to find the generalized inverse of the matrix, $\mathbf{P}_{\mathbf{H}}^{\perp} = \mathbf{I} - \mathbf{H}(\mathbf{H}^{\mathrm{H}}\mathbf{H})^{-1}\mathbf{H}^{\mathrm{H}}$ is the orthogonal complement space of $\mathbf{H}$. $\mathbf{B_{SH}}$ has the following properties:

$$\mathbf{B_{SH}}\mathbf{S} = \mathbf{S}, \quad \mathbf{B_{SH}}\mathbf{H} = \mathbf{0}. \tag{17}$$

The mainlobe interference subspace $\mathbf{E}_{\mathrm{m}} = [\mathbf{a}(\hat{\theta}_1)]$, and the joint subspace $\mathbf{E}_{\mathrm{sp}} = [\mathbf{a}(\hat{\theta}_0), \mathbf{a}(\hat{\theta}_2), \ldots, \mathbf{a}(\hat{\theta}_p)]$ of the desired signal and sidelobe interferences are established by the estimated signal steering vectors respectively. There is no intersection between the subspaces due to the different directions of the desired signal and the interferences. The subspace $\mathbf{E}_{\mathrm{m}}$ is projected onto the subspace $\mathbf{E}_{\mathrm{sp}}$, the oblique projection operator at this point can be expressed as:

$$\mathbf{B} = \mathbf{E}_{\mathrm{sp}}(\mathbf{E}_{\mathrm{sp}}^{\mathrm{H}}\mathbf{P}_{\mathrm{m}}^{\perp}\mathbf{E}_{\mathrm{sp}})^{-1}\mathbf{E}_{\mathrm{sp}}^{\mathrm{H}}\mathbf{P}_{\mathrm{m}}^{\perp} \tag{18}$$

where $\mathbf{P}_{\mathrm{m}}^{\perp} = \mathbf{I} - \mathbf{E}_{\mathrm{m}}(\mathbf{E}_{\mathrm{m}}^{\mathrm{H}}\mathbf{E}_{\mathrm{m}})^{-1}\mathbf{E}_{\mathrm{m}}^{\mathrm{H}}$ is the orthogonal complement space of $\mathbf{E}_{\mathrm{m}}$. From (17), we can obtain:

$$\begin{cases} \mathbf{B} \cdot \mathbf{E}_{\mathrm{sp}} = \mathbf{E}_{\mathrm{sp}} \\ \mathbf{B} \cdot \mathbf{E}_{\mathrm{m}} = \mathbf{0} \end{cases} \rightarrow \begin{cases} \mathbf{B} \cdot \mathbf{a}(\hat{\theta}_0) = \mathbf{a}(\hat{\theta}_0), \\ \mathbf{B} \cdot \mathbf{a}(\hat{\theta}_1) = \mathbf{0}, \\ \mathbf{B} \cdot \mathbf{a}(\hat{\theta}_i) = \mathbf{a}(\hat{\theta}_i), i = 2, \ldots, p. \end{cases} \tag{19}$$

Assuming that the DOA estimation of each signal is accurate, then $\mathbf{B}$ can be used to filter out the mainlobe interference in the training data:

$$\mathbf{Y} = \mathbf{BX}. \tag{20}$$

Based on the reconstructed SINCM and (4), the adaptive weight vector can be expressed as:

$$\omega_{\mathrm{re}} = \frac{\hat{\mathbf{R}}_{i+n}^{-1}\mathbf{a}(\hat{\theta}_0)}{\mathbf{a}(\hat{\theta}_0)^{\mathrm{H}}\hat{\mathbf{R}}_{i+n}^{-1}\mathbf{a}(\hat{\theta}_0)}. \tag{21}$$

Then the output of the adaptive beamformer is calculated as:

$$\mathbf{Z} = \omega_{\mathrm{re}}^{\mathrm{H}}\mathbf{Y} = \omega_{\mathrm{re}}^{\mathrm{H}}\mathbf{BX}. \tag{22}$$

The processing block diagram of the proposed method is described in Fig. 3, which can effectively suppress mainlobe and sidelobe interferences only by knowing the prior information of the array structure and the angular sector where the desired signal is located, even if the desired signal exists in the received signal. This method relies on the accurate estimation of signal DOA, and the TROMP algorithm proposed in this paper can effectively solve the problem of inaccurate estimation of DOA when both the desired signal and mainlobe interference exist in the received signal, so that the adaptive weight vector ω_{re} and oblique projection operator $\mathbf{B}$ can be calculated.

4. Simulations and Verification

Assuming that the uniform linear array is composed of 16 elements, and the spacing of array elements is a half wavelength. The direction of the desired signal is 0° with signal-to-noise ratio (SNR) 5 dB. The interferences include one mainlobe interference and two sidelobe interferences. The direction of the mainlobe interference is 3° and the interference-to-noise ratio (INR) is 20 dB. The directions of sidelobe interferences are −20° and 30° with INR 30 dB and 35 dB, respectively.
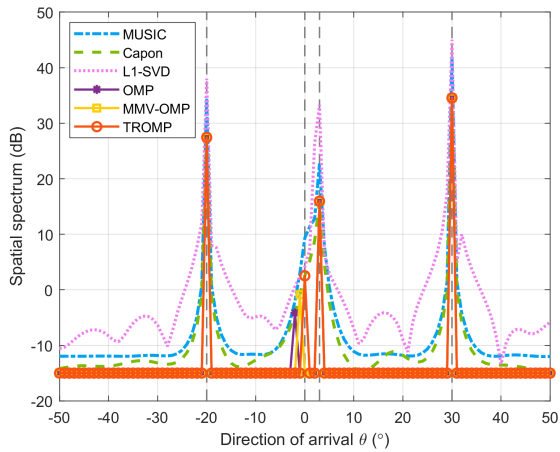
Fig. 4. Comparison of DOA estimation.

4.1 Comparison of DOA Estimation Performance

The TROMP algorithm is compared to Capon, MUSIC, OMP, L1-SVD [26] and MMV-OMP [27]. The DOA estimation result is obtained from one Monte Carlo experiment, and the DOA successful estimation probability is calculated from an average of 200 independent Monte Carlo experiments. The space is uniformly divided into 181 angles, i.e., $\Delta = 1°$, suppose the desired signal is known to exist in $[-2°, 2°]$. The snapshot number of MUSIC, Capon and L1-SVD are 50, both OMP and TROMP are single snapshot, and the snapshot number of MMV-OMP is 5. The threshold factor m of TROMP is 3. Since OMP, TROMP and MMV-OMP cannot obtain the power estimation of signal, for the convenience of comparison, the signal steering vector calculated by OMP, TROMP and MMV-OMP is substituted into (6), then the power of signal in this direction can be obtained, and the power in other no signal directions is set as the minimum power of Capon spectrum. Figure 4 shows the DOA estimation result of six algorithms.

It can be seen from Fig. 4 that when the snapshot number is not large enough and the intensity of the mainlobe interference is obviously greater than the desired signal, the DOA estimation results of MUSIC, Capon and L1-SVD for the desired signal are not clear. OMP and MMV-OMP can estimate the DOAs of interferences successfully, but the estimation of the desired signal is biased. While the TROMP algorithm accurately estimates the DOAs of four signals. Combined with the known desired signal angular sector, the desired signal and interferences can be distinguished from the TROMP algorithm results.

Figure 5 compares the probabilities of successful DOA estimation of the above algorithms under different SNR. The successful estimation means that effective peaks can be formed in all signal directions, and the sum of DOA estimation deviations of all signals does not exceed 1°, that is, the DOA estimation of at most one signal is allowed to deviate by 1°. The SNR of the desired signal is set to be 0 ~ 10 dB.
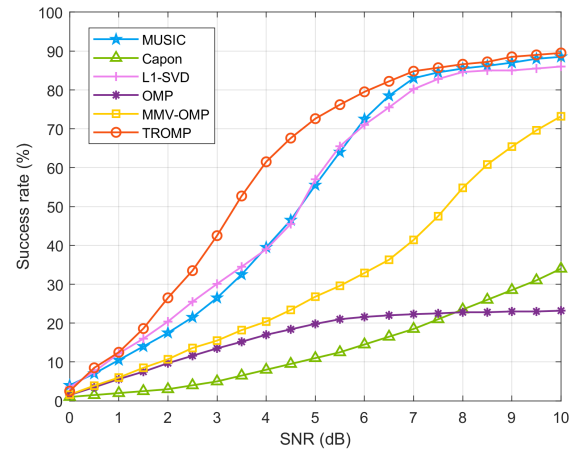
Fig. 5. The probabilities of successful DOA estimation.

Algorithm	Computational cost	Time consumption
Capon	$O((2N + K)M^2)$	0.0695
MUSIC	$O((2N + K)M^2)$	0.0744
L1-SVD	$O(PN^3)$	0.3315
OMP	$O(PMN)$	0.0086
MMV-OMP	$O(PKMN)$	0.0245
TROMP	$O\left(PM\left(N + 4mP^2\right)\right)$	0.0156

Tab. 1. Comparison of computational complexity and time consumption.

As can be seen from Fig. 5, with the increase of SNR, DOA successful estimation probabilities of six algorithms also increase gradually. When the SNR increases to 10 dB, MUSIC, L1-SVD and TROMP have high probability of success in estimation. And the estimation performance of TROMP is always better than MUSIC and L1-SVD, especially in the case of low SNR. The estimation performance of MMV-OMP increases rapidly when the SNR is greater than 7 dB. While the estimated success probability of Capon and OMP is far less than that of the other four algorithms.

For M array elements and P signal sources, the divided grids is N and the snapshot number of Capon, MUSIC, L1-SVD and MMV-OMP is K. Table 1 lists the simplified computational complexity and time consumption of one DOA estimation of the above algorithms, where the values of each parameter in the time consumption are stated in the simulation conditions. The computational cost of TROMP algorithm is between OMP and MMV-OMP, and less than Capon, MUSIC and L1-SVD. The hardware environment used in this study includes an Intel i5-8500 CPU operating at 3.0 GHz and 16 GB of RAM.

4.2 Comparison of Interference Suppression Performance

The proposed method is compared to SMI, EMP, EMP-CMR [9], EMP-SC [10], and EOMP-CMR [13]. The adaptive beam pattern is obtained from one Monte Carlo experiment and the output signal-to-interference-plus-noise ratio (SINR) is calculated from an average of 200 independent
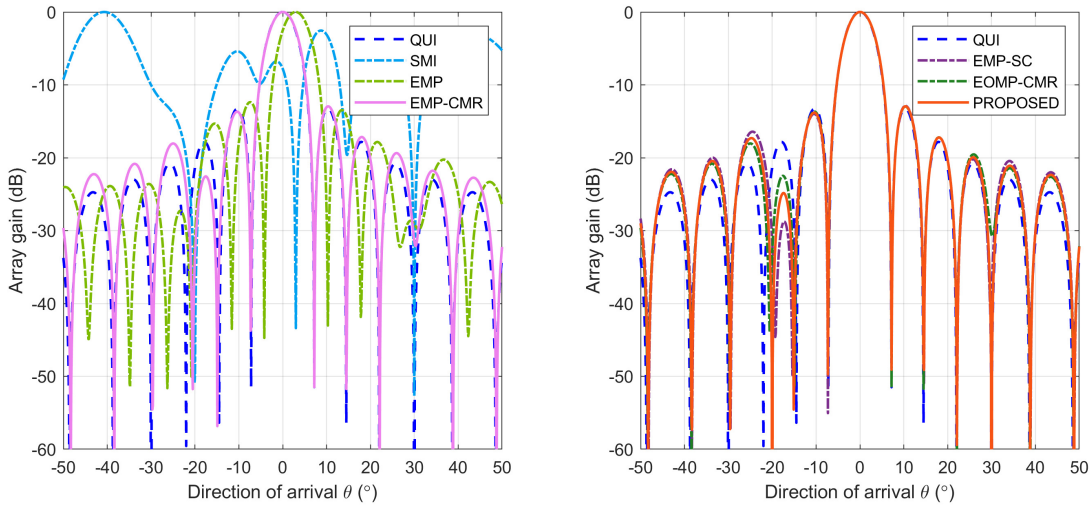
Fig. 6. Adaptive beam patterns comparison.

Monte Carlo experiments. In Fig. 6, beam patterns of all mentioned methods are shown, and compared with the quiescent (QUI) beam pattern. The snapshot number is 100. For better comparison, the desired signal is not present in the training data when using EMP, EMP-CMR and EMP-SC methods, and assuming that EOMP-CMR knows the direction of the desired signal in advance.

As can be seen from Fig. 6, SMI form deep null in the mainlobe that causes mainlobe distortion. EMP suffers from the peak offset. When there is no desired signal in the training data, EMP-CMR and EMP-SC can effectively solve the problem of beam peak deviation. But the snapshot number is relatively small leads to the EMP-CMR formed null at 30° is not deep enough. The beam pattern of EOMP-CMR and the proposed method can effectively solve the mainlobe distortion and offset, and deep nulls are formed in the directions of sidelobe interferences.

Figure 7 shows the output SINRs of the aforementioned methods versus the snapshot number which ranges from 10 ~ 100. As can be seen from Fig. 7, the proposed method's output SINR is similar to EMP-CMR, EMP-SC and EOMP-CMR. Due to the high accuracy of TROMP in DOA estimation, the proposed method can also have well performance in low snapshot numbers. In addition, compared with the EMP-CMR, EMP-SC and EOMP-CMR, the output SINR of the proposed method has a faster convergence rate.

Figure 8 depicts the output SINRs curves of all mentioned methods when the mainlobe interference INR varies from 10 dB to 60 dB, and the number of snapshots is 100. It can be seen from Fig. 8 that compared with other methods, the output SINR of the proposed method is higher, and the curve decreases more slowly with the increase of the mainlobe interference INR. It shows that the proposed method is less affected by the mainlobe interference intensity and has better interference suppression performance.
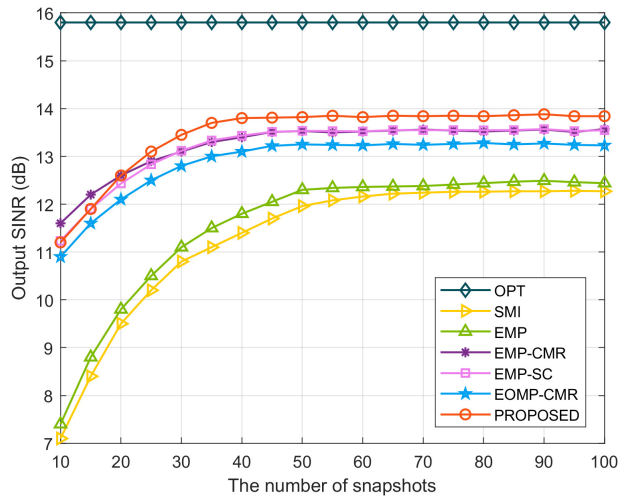
Fig. 7. Output SINRs versus the number of snapshots.
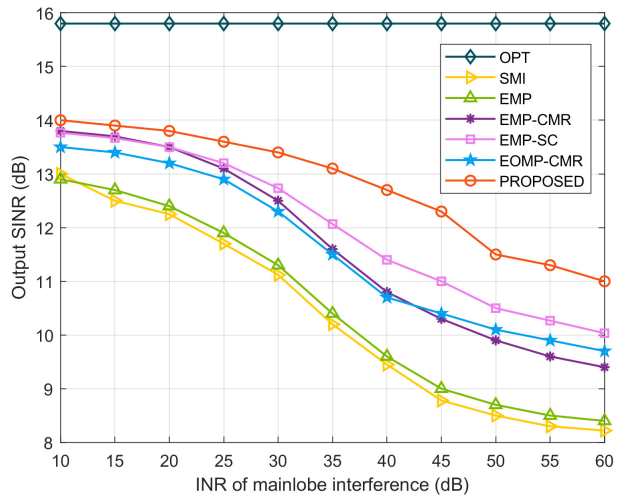
Fig. 8. Output SINRs versus the INR of mainlobe interference.

5. Conclusion

In this paper, we propose a novel mainlobe interference suppression method based on compressive sensing and covariance matrix reconstruction. The DOAs of the signals can be accurately estimated by the proposed TROMP algorithm, and then the SINCM is reconstructed and the oblique projection operator is calculated. Finally, the mainlobe interference and sidelobe interferences are effectively suppressed while the desired signal exists in the received signal. The simulation demonstrates that the TROMP algorithm has excellent performance in estimating the signal DOA, which ensures the effectiveness of the subsequent steps of suppressing the interferences. In addition, the adaptive beam pattern formed by the proposed mainlobe interference suppression method has no distortion or offset, which can obtain better filtering performance and robustness compared with other methods.

At present, the application of the proposed method in mitigating multi-mainlobe interferences is still under discussion. In the future research, we will combine the TROMP algorithm with Multiple Measurement Vectors, and explore the more effective multi-main lobe interferences suppression method.

Acknowledgments

References

[1] BUTT, F. A., JALIL, M. An overview of electronic warfare in radar systems. In *The International Conference on Technological Advances in Electrical, Electronics and Computer Engineering (TAEECE)*. Konya (Turkey), 2013, p. 213–217. DOI: 10.1109/TAEECE.2013.6557273.

[2] TONG, X. Modeling and realization of real time electronic countermeasure simulation system based on SystemVue. *Defence Technology*, 2020, vol. 16, no. 2, p. 470–486. DOI: 10.1016/j.dt.2019.08.010

[3] CHEN, X., SHU, T., YU, K.-B., et al. Joint adaptive beamforming techniques for distributed array radars in multiple mainlobe and sidelobe jammings. *IEEE Antennas and Wireless Propagation Letters*, 2019, vol. 19, no. 2, p. 248–252. DOI: 10.1109/LAWP.2019.2958687

[4] GE, M., CUI, G., YU, X., et al. Mainlobe jamming suppression with polarimetric multi-channel radar via independent component analysis. *Digital Signal Processing*, 2020, vol. 106, p. 1–11. DOI: 10.1016/j.dsp.2020.102806

[5] LU, Y., MA, J., SHI, L., et al. Multiple interferences suppression with space-polarization null-decoupling for polarimetrie array. *Journal of Systems Engineering and Electronics*, 2021, vol. 32, no. 1, p. 44–52. DOI: 10.23919/JSEE.2021.000006

[6] GUO, S., WANG, J., CHEN, G., et al. Mainlobe interference suppression based on independent component analysis in passive bistatic radar. *IET Signal Processing*, 2018, vol. 9, no. 12, p. 1193–1201. DOI: 10.1049/iet-spr.2018.5198

[7] ZHOU, B., LI, R., LIU, W., et al. A BSS-based space-time multi-channel algorithm for complex-jamming suppression. *Digital Signal Processing*, 2019, vol. 87, p. 86–103. DOI: 10.1016/j.dsp.2019.01.007

[8] LI, R., WANG, Y., WAN, S. Research of reshaping adapted pattern under mainlobe interference conditions. *Modern Radar*, 2002, vol. 24, no. 3, p. 50–53. DOI: 10.3969/j.issn.1004-7859.2002.03.015

[9] YANG, X., ZHANG, Z., ZENG, T., et al. Mainlobe interference suppression based on eigen-projection processing and covariance matrix reconstruction. *IEEE Antennas and Wireless Propagation Letters*, 2014, vol. 13, p. 1369–1372. DOI: 10.1109/LAWP.2014.2339224

[10] QIAN, J., HE, Z. Mainlobe interference suppression with eigenprojection algorithm and similarity constraints. *Electronics Letters*, 2016, vol. 52, no. 3, p. 228–230. DOI: 10.1049/el.2015.2951

[11] MALLIPEDDI, R., LIE, J., RAZUL, S. G., et al. Robust adaptive beamforming based on covariance matrix reconstruction for look direction mismatch. *Progress In Electromagnetics Research Letters*, 2011, vol. 25, p. 37–46. DOI: 10.2528/PIERL11040104

[12] GU, Y., LESHEM, A. Robust adaptive beamforming based on interference covariance matrix reconstruction and steering vector estimation. *IEEE Transactions on Signal Processing*, 2017, vol. 60, no. 7, p. 3881–3885. DOI: 10.1109/TSP.2012.2194289

[13] GAO, S., ZHANG, C., YANG, X., et al. Adaptive beamforming based on eigen-oblique projection for mainlobe interference suppression. In *IEEE International Conference on Signal, Information and Data Processing (ICSIDP)*. Chongqing (China), 2019, p. 1–4. DOI: 10.1109/ICSIDP47821.2019.9173405

[14] JI, Y., LU, Y., WEI, S., et al. Multiple mainlobe interferences suppression based on eigen-subspace and eigen-oblique projection. *Sensors*, 2022, vol. 22, no. 21, p. 1–12. DOI: 10.3390/s22218494

[15] LUO, Z., WANG, H., LV, W., et al. Mainlobe anti-jamming via eigen-projection processing and covariance matrix reconstruction. *IEICE Transactions on Fundamentals of Electronics, Communications and Computer Sciences*, 2017, vol. 100, no. 4, p. 1055–1059. DOI: 10.1587/transfun.E100.A.1055

[16] WANG, Y., BAO, Q., CHEN, Z. Robust mainlobe interference suppression for coherent interference environment. *EURASIP Journal on Advances in Signal Processing*, 2016, vol. 135, p. 1–7. DOI: 10.1186/s13634-016-0434-z

[17] GU, Y., GOODMAN, N. A., HONG, S., et al. Robust adaptive beamforming based on interference covariance matrix sparse reconstruction. *Signal Processing*, 2014, vol. 96, part B, p. 375–381. DOI: 10.1016/j.sigpro.2013.10.009

[18] LI, X., YU, B., HUANG, P. Mainlobe interference suppression via eigen-projection processing and covariance matrix sparse reconstruction. *IEICE Electronics Express*, 2018, vol. 15, no. 17, p. 1–8. DOI: 10.1587/elex.15.20180683

[19] HADI, M. A., ALSHEBEILI, S., JAMIL, K., et al. Compressive sensing applied to radar systems: An overview. *Signal, Image and Video Processing*, 2015, vol. 9, p. 25–39. DOI: 10.1007/s11760-015-0824-y

[20] CHEN, S., CHENG, Z., LIU, C., et al. A blind stopping condition for orthogonal matching pursuit with applications to compressive sensing radar. *Signal Processing*, 2019, vol. 165, p. 331–342. DOI: 10.1016/j.sigpro.2019.07.022

[21] DING, L., LI, R., DAI, L., et al. Discrimination and identification between mainlobe repeater jamming and target echo via sparse recovery. *IET Radar, Sonar & Navigation*, 2019, vol. 11, no. 2, p. 235–242. DOI: 10.1049/iet-rsn.2016.0109

[22] GE, M., CUI, G., YU, X., et al. Main lobe jamming suppression via blind source separation sparse signal recovery with subarray configuration. *IET Radar, Sonar & Navigation*, 2020, vol. 14, no. 3, p. 431–438. DOI: 10.1049/iet-rsn.2019.0500

[23] RANI, M., DHOK, S. B., DESHMUKH, R. B. A systematic review of compressive sensing: Concepts, implementations and applications. *IEEE Access*, 2018, vol. 6, p. 4875–4894. DOI: 10.1109/ACCESS.2018.2793851

[24] TROPP, J. A., GILBERT, A. C. Signal recovery from random measurements via orthogonal matching pursuit. *IEEE Transactions on Information Theory*, 2007, vol. 53, no. 12, p. 4655–4666. DOI: 10.1109/TIT.2007.909108

[25] WANG, W., WU, R. High resolution direction of arrival (DOA) estimation based on improved orthogonal matching pursuit (OMP) algorithm by iterative local searching. *Sensors*, 2013, vol. 9, no. 13, p. 11167–11183. DOI: 10.3390/s130911167

[26] MALIOUTOV, D., CETIN, M., WILLSKY, A. S. A sparse signal reconstruction perspective for source localization with sensor arrays. *IEEE Transactions on Signal Processing*, 2005, vol. 53, no. 12, p. 3010–3022. DOI: 10.1109/TSP.2005.850882

[27] LI, Y., CHI, Y. Off-the-grid line spectrum denoising and estimation with multiple measurement vectors. *IEEE Transactions on Signal Processing*, 2016, vol. 64, no. 5, p. 1257–1269. DOI: 10.1109/TSP.2015.2496294

About the Authors . . .

Xinpeng ZHAO was born in 2000. He is currently pursuing the master's degree in Electronic Science and Technology with the School of Electronic Engineering, Xidian University. His research interests include adaptive array signal and compressive sensing.

Aifeng REN (corresponding author) was born in 1974. He received his Ph.D. degree from Xi'an Jiaotong University. He is currently a Professor with the School of Electronic and Engineering, Xidian University. His research interests include embedded wireless sensor networks, terahertz sensing technology, complex brain networks, and signal and image processing.